Antarctic Science 32(5), 408–424 (2020) © Antarctic Science Ltd 2020 doi:10.1017/S0954102020000255

Winter climate change on the northern and southern Antarctic Peninsula

OLEKSANDR M. EVTUSHEVSKY[1], VOLODYMYR O. KRAVCHENKO[1], ASEN V. GRYTSAI[2] and GENNADI P. MILINEVSKY[1,3,4]

[1]Space Physics Laboratory, Taras Shevchenko National University of Kyiv, 64/13 Volodymyrska Street, 01601 Kyiv, Ukraine
[2]Astronomy and Space Physics Department, Taras Shevchenko National University of Kyiv, 64/13 Volodymyrska Street, 01601 Kyiv, Ukraine
[3]International Center of Future Science, Jilin University, 2699 Qianjin Street, 130012 Changchun, China
[4]Department of Atmosphere Physics, National Antarctic Scientific Center, 16 Taras Shevchenko Boulevard, 01601 Kyiv, Ukraine
o_evtush@ukr.net

Abstract: Differences in the decadal trend in the winter surface temperature in the northern and southern Antarctic Peninsula have been analysed. Time series from the two stations Esperanza and Faraday/Vernadsky since the early 1950s are used. The two time series are strongly correlated only during the 1980s and 1990s when their variability and trends are associated with both the Niño-4 region and Southern Annular Mode impacts. The winter cooling at the Faraday/Vernadsky station contrasts with the winter warming at the Esperanza station during the period of 2006–17. The different temperature trends are accompanied by weak correlations between the temperatures at these two stations. Linearly congruent components of the station temperature trends in 2006–17 indicate a dominant contribution of Southern Annular Mode (tropical sea surface temperature anomalies) to warming (cooling) in the northern (southern) Peninsula. Distinctive impacts of climate modes are observed in combination with the recent deepening of the negative sea-level pressure anomaly to the west of the peninsula and the related change in the zonal and meridional wind components. These factors apparently contribute to the occurrence of the boundary that crosses the peninsula and divides it into sub-regions with warming and cooling.

Received 7 July 2018, accepted 13 April 2020

Key words: Annular Mode, El Niño, planetary waves, READER database, surface temperature, zonal and meridional wind

Introduction

Meteorological observations on the stations of the Antarctic Peninsula (AP) showed rapid climate warming in the second half of the twentieth century. There were differences in the temperature trends on the western and eastern sides of the AP as well as in winter and summer. The largest temperature increase was observed in winter (June–August) in the western Peninsula, and it reached ~5°C between the 1950s and early 2000s (Vaughan *et al.* 2003, Turner *et al.* 2005). Recently, a change in temperature trend sign has been diagnosed with a cooling tendency since the late 1990s–early 2000s (Carrasco 2013, Turner *et al.* 2016, 2019, Oliva *et al.* 2017). As indicated by the arrow in Fig. 1a, the peak value in the winter temperature increase in the Southern Hemisphere (SH) in the 55 year period (1951–2005) is 5°C, and it is located in the region of the western and southern AP. Data from the NASA Goddard Institute for Space Science (GISS) Surface Temperature Analysis are used (Hansen *et al.* 2010). The temperature increase over 1951–2005 is 1–3°C on the rest of the AP and over West Antarctica (red in Fig. 1a).

In the annual mean temperature, the last decade (2006–15) was cooler than the preceding one (1996–2005) for most AP stations (Oliva *et al.* 2017). The cooling in the annual mean temperature in the last decade was mainly due to negative trends in spring and summer (Fig. S1g & h in Supplemental Material). This is generally consistent with Carrasco (2013), Turner *et al.* (2016) and Oliva *et al.* (2017). The trend was slightly positive across the AP in autumn (Fig. S1i). The winter warming tendency (Fig. 1a) has changed to the cooling tendency in most of the Antarctic regions (by 1–2°C; blue in Fig. 1b), except at the northern tip of the AP, where warming continued and the temperature increased by ~2°C (indicated by arrows in Fig. 1b). Seasonal diversity of temperature change over the AP in 2006–17 (Fig. S1f–i) contrasts with seasonally persistent warming in 1951–2005 (Fig. S1a–d). In annual means, strong warming (Fig. S1e) and weak cooling (Fig. S1j) were observed over the AP in the preceding and recent periods, respectively.

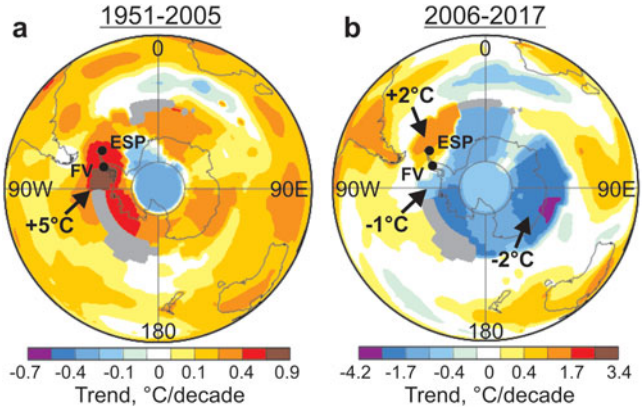

Fig. 1. Decadal trends of the surface temperature in the Southern Hemisphere winter, June–August. **a.** The 55 year period from 1951 to 2005. **b.** The 12 year period from 2006 to 2017. Antarctic stations Esperanza (ESP) and Faraday/Vernadsky (FV) are shown by closed circles. The arrows indicate the total temperature changes in the Antarctic Peninsula region over the specified periods. Data from the NASA Goddard Institute for Space Science Surface Temperature Analysis.

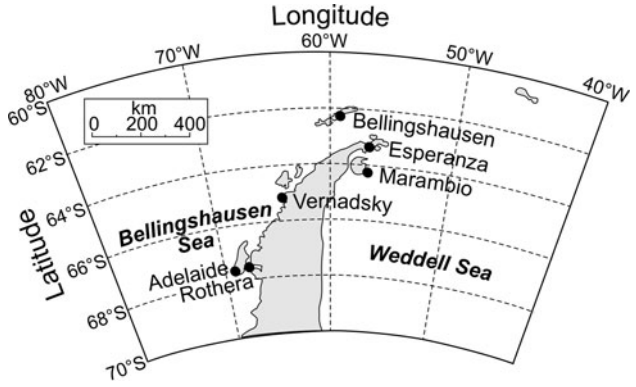

Fig. 2. Location map of the weather stations in the Antarctic Peninsula region.

It has been established that warming in West Antarctica in winter and spring was associated with tropical influences due to increasing sea surface temperatures (SSTs) in the central Pacific (Ding *et al.* 2011, Schneider *et al.* 2012, Clem & Fogt 2013), while the summer warming in the AP region was mainly due to the strengthening of zonal circulation and the positive trend in the Southern Annular Mode (SAM) (Marshall *et al.* 2006) attributed to increasing levels of greenhouse gases (Kushner *et al.* 2001) and the ozone hole influence (Thompson *et al.* 2011).

Effects of the tropical anomalies and SAM vary spatially across the AP, and interaction between the main modes of climate variability influences the AP climate change on the decadal timescale (Marshall 2007, Yu *et al.* 2012, Clem & Fogt 2013, Clem *et al.* 2016). Decadal periodicity in the AP temperature has been revealed by Kravchenko *et al.* (2011). In this work, we analyse the winter temperature variations in the northern AP (NAP) and southern AP (SAP). Decadal changes in the co-variability between them and their associations with zonal and meridional winds, with the El Niño and Annular Mode indices and with sea-level pressure (SLP) anomalies are examined.

Data description and analysis method

We have created five time series ending in 2017 for the winter temperatures (June–August) measured at the AP weather stations (Fig. 2) using the Scientific Committee on Antarctic Research (SCAR) Reference Antarctic Data for Environmental Research (READER). The SCAR READER project data (Turner *et al.* 2004) are available at www.antarctica.ac.uk/met/READER. The stations are Bellingshausen (BEL), Esperanza (ESP) and Marambio (MAR) for the NAP and Vernadsky and Rothera (ROT) for the SAP. The Vernadsky station (since 1996) is the former Faraday station, and the common time series named as Faraday/Vernadsky (FV) starts from 1951. Data from ROT (since 1977) are combined with data from nearby station Adelaide (1962–74) in the Adelaide–ROT (AR) time series.

The five time series are shown in Fig. 3, separately for the SAP (Fig. 3a & b) and NAP (Fig. 3c–e) stations. Time series lengths are also indicated in Fig. 3 next to the names of the stations. Station temperatures for the SAP and NAP regions are correlated with one another at $r \geq 0.9$ (indicated in Fig. 3), but the SAP *vs* NAP correlation is much lower at $r = 0.5$–0.7 (Table I).

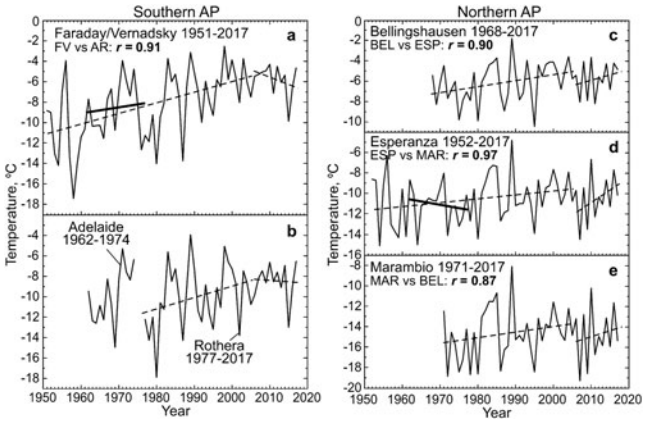

Fig. 3. Time series of the winter temperatures at the stations of the southern Antarctic Peninsula (AP): **a.** Faraday/Vernadsky (FV) and **b.** Adelaide–Rothera (AR); and the northern AP: **c.** Bellingshausen (BEL), **d.** Esperanza (ESP) and **e.** Marambio (MAR). Dashed (thick solid) lines show piecewise linear trends before and after 2005 (in the 1960s–1970s). Correlation coefficients r between time series are indicated.

https://doi.org/10.1017/S0954102020000255 Published online by Cambridge University Press

Table I. Correlations between the winter temperature time series obtained at the stations of the southern Antarctic Peninsula (SAP; Faraday/Vernadsky and Adelaide–Rothera) and northern Antarctic Peninsula (NAP; Bellingshausen, Esperanza and Marambio).

	NAP stations		
SAP stations	Bellingshausen	Esperanza	Marambio
Faraday/Vernadsky	0.65	0.56	0.46
Adelaide–Rothera	0.69	0.52	0.50

Similarly, decreasing correlations with increasing distance between the AP stations were found in previous studies (King 1994, Kravchenko *et al.* 2011, Oliva *et al.* 2017, Turner *et al.* 2019).

In other works, the temperatures on different parts of the peninsula (western, eastern, northern and southern) are analysed separately or are compared, in view of the differences in the local influences related to zonal circulation and individual climate modes (King 1994, Vaughan *et al.* 2003, Turner *et al.* 2005, Stastna 2010, Clem & Fogt 2013, van Wessem *et al.* 2015, Oliva *et al.* 2017). Such a division of the NAP and SAP has been used before (Clem & Fogt 2013, van Wessem *et al.* 2015, Oliva *et al.* 2017, Turner *et al.* 2019). We follow these studies and classify the same stations (Fig. 2) as the NAP and SAP, respectively, based on the opposite temperature trends in 2006–17 (shown by arrows in Fig. 1b).

It is known that global temperatures exhibit differing trends during different periods with both piecewise linear behaviour and step-like changes (e.g. Seidel & Lanzante 2004). Figures 1, 3, S1 and S2 illustrate the changing nature of the temperature trends in the AP region. We use the piecewise linear trend method with a sloped steps model, incorporating both abrupt changes and slopes during the periods between breakpoints (Seidel & Lanzante 2004). Dashed lines in Fig. 3 show the piecewise linear trends with the sloped steps for the periods before 2005 and since 2006 (the reference periods are defined in the Results).

Given the high correlation between the SAP stations, as well as between the NAP stations, we use the two longest time series, namely FV (1951–2017, 67 years; Fig. 3a) and ESP (1952–2017, 66 years; Fig. 3d), respectively, in correlative relationships as representative of each of the two AP sub-regions. The statistical significance of linear trends, linear correlations and linear regression was estimated using Student's *t*-test. Running correlation with the 10 year window was used to detect interannual and decadal temperature variability.

Surface temperature trends in the SH (Figs 1 & S1) are illustrated by the trend maps using the data from the NASA GISS Surface Temperature Analysis (https://data.giss.nasa.gov/gistemp/maps; Hansen *et al.* 2010).

Table II. Temperature trends (in °C decade^{-1}) at the northern Antarctic Peninsula (NAP) and southern Antarctic Peninsula (SAP) stations before and after 2005. Time series size (in years) is in parentheses.

	Station, starting year	Before 2005	2006–17 (12)
NAP	Bellingshausen, 1968	0.56 ± 0.55[a] (38)	1.21 ± 2.80
NAP	Esperanza, 1952	0.32 ± 0.39[b] (54)	1.95 ± 3.80[c]
NAP	Marambio, 1971	0.58 ± 0.84 (35)	1.24 ± 4.71
SAP	Faraday/Vernadsky, 1951	1.05 ± 0.50[a] (55)	-1.46 ± 2.54[c]
SAP	Adelaide–Rothera, 1962	1.12 ± 1.35[b] (44)	-0.28 ± 3.10

[a]Significant at the confidence limit of 95%.
[b]Significant at the confidence limit of 90%.
[c]Significant at the confidence limit of 70%.

To analyse the association between the AP temperatures and the meteorological variables on the regional and hemispheric scales, the data from the National Centers for Environmental Prediction (NCEP)–National Center for Atmospheric Research (NCAR) reanalysis (NNR; www.esrl.noaa.gov/psd) (Kalnay *et al.* 1996) are used. The NNR provides various analysis tools, and we have plotted the maps of the linear correlation between the AP temperature time series and the winter averages of the NNR gridded variables (www.esrl.noaa.gov/psd/data/correlation). Individual NNR time series (dashed lines in Fig. S2) are compared with those from ERA Interim (ERA hereafter; dotted lines; https://apps.ecmwf.int/datasets/data/interim-full-moda/levtype=sfc) available since 1979 (Dee *et al.* 2011). As demonstrated in Fig. S2, both reanalyses reliably reproduce the temperature variability and tendencies at ESP and FV with high correlations with the observed temperatures ($r = 0.8$–0.9), although the difference in mean values reaches a few degrees. Recent NAP warming of the order of 2°C decade^{-1} agrees between the time series (Fig. S2 and ESP row in Table SI), and reanalyses show much weaker SAP cooling than has been observed (Fig. S2b and FV row in Table SI). In the latter case, negative trends from the reanalyses are close to the trend at ROT (Table II) and demonstrate the absence of SAP warming in 2006–17. In general, this comparison gives a reason to use the reanalysis data in the analysis of spatial and temporal changes in the AP climate. Note that both reanalyses are widely used in the study of Antarctic climate variability and trends (Marshall 2003, Clem & Fogt 2013, Wang *et al.* 2016, Turner *et al.* 2019, Yu *et al.* 2020).

The possible decadal changes in the influences of the main modes of climate variability on the AP climate (noted in the Introduction) were estimated using individual climate indices (Fig. S3). Among the El Niño indices, the Niño-4 (N4) index, available since 1948 in the NNR data (www.esrl.noaa.gov/psd/data/correlation/nina4.data), has been chosen, as argued in the Results.

https://doi.org/10.1017/S0954102020000255 Published online by Cambridge University Press

For the Annular Mode, the Marshall SAM index and Antarctic Oscillation (AAO) index were used. The SAM index is based on the station data and describes the zonal mean surface pressure difference between the latitudes of 40°S and 65°S since 1957 (https://legacy.bas.ac.uk/met/gjma/sam.html; Marshall 2003). The AAO index is defined as the leading mode of Empirical Orthogonal Function analysis of the 700 hPa height anomalies south of 20°S (Mo 2000) and is available at www.cpc.ncep.noaa.gov/products/precip/CWlink/daily_ao_index/aao/aao.shtml.

The part of the ESP or FV temperature trend contributed by the trend in the wind component or climate mode was estimated by the method of congruent trend (Thompson *et al.* 2000, Yang *et al.* 2016). The station temperature trend that is linearly congruent with the examined variable trend was found as a product of the coefficient of the linear regression between the two time series and linear trend in the examined variable. As in Yang *et al.* (2016), the de-trended time series were used in the regression analysis.

Both consistent and contrasting temperature trends on the NAP and SAP persisted for more than one decade (Figs 1, 3 & S1) and played significant roles in regional climate changes. In the following sections, we offer an explanation of these similarities and differences.

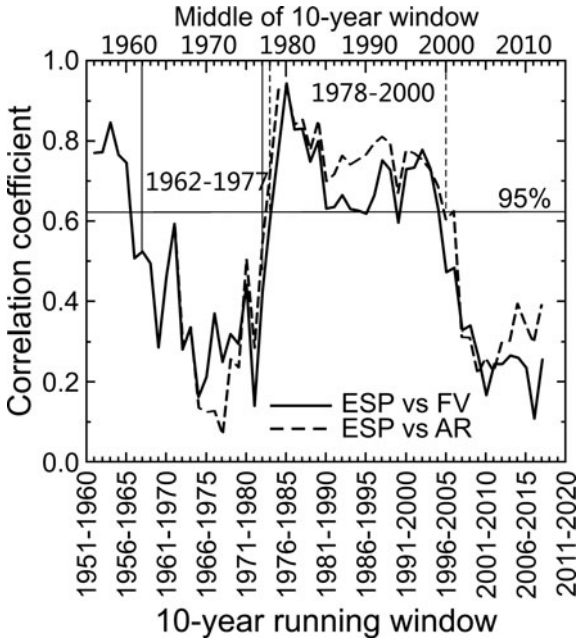

Fig. 4. Running correlation with a 10 year window between the temperature time series of Esperanza (ESP) and Faraday/Vernadsky (FV; solid curve) and Adelaide–Rothera (AR; dashed curve). Horizontal line indicates the 95% confidence limit for the 10 year correlation ($r = 0.62$).

Results

Correlative relationships

As seen in Figs 1 & 3 and Table II, the temperature trends along the AP are consistently positive before *c.* 2005 and differ later. In particular, the warming (cooling) tendency in the NAP (SAP) region in 2006–17 is observed. The piecewise linear trends show a change from the positive to negative slope in the SAP time series in the 2000s (dashed lines in Fig. 3a & b). At the same time, a stepwise temperature decrease with continued warming is seen from the NAP time series (dashed lines in Fig. 3c–e). The statistical significance of the ESP and FV temperature trend in 2006–17 reaches the 70% confidence level (Table II). While the trend values in the NAP and SAP time series are of relatively low statistical significance in 2006–17, the signs of the trends are consistent within the sub-regions (Fig. 3 & Table II).

We have examined a change with time in the co-variability between the temperature time series for ESP (NAP) and FV (SAP). Running correlation with a 10 year window shows that substantial multi-decadal changes occur in the value and statistical significance of the correlation coefficient (solid curve in Fig. 4, horizontal line indicates the 95% confidence limit). The upper horizontal axis in Fig. 4 indicates the centres of the 10 year windows. Statistically significant correlations are observed in the late 1950s and between 1980 and 2000. The correlation between the ESP time series and the shorter one for AR (dashed curve in Fig. 4) completely reproduces decadal changes in the ESP *vs* FV relationship (solid curve).

The periods of the 1960s–1970s and the 2000s–2010s are characterized by low correlations that suggest the absence of the common factors influencing the NAP and SAP temperatures. As noted from Figs 1b & 3 and Table I, the NAP and SAP sub-regions undergo opposite climatic tendencies in the period of low correlation of the 2000s–2010s.

Note that the first period of low correlation in Fig. 4 (the 1960s–1970s) is also characterized by opposing trends in NAP and SAP, although they are not statistically significant at the 90% confidence level. The corresponding positive trend for FV and negative trend for ESP are shown by thick lines in Fig. 3a & d, respectively. Estimates were made for the 16 year period from 1962 to 1977 (Fig. 4, solid vertical lines from the upper horizontal axis, where the central years of the 10 year running windows are indicated). It is seen in Fig. 3 that warming (FV) and cooling (ESP) tendencies in 1962–77 are the reverse of those after 2000. This indicates that different factors can cause interruptions to the co-variability between the NAP and SAP temperatures in different decades.

https://doi.org/10.1017/S0954102020000255 Published online by Cambridge University Press

As can be seen from the distance scale in Fig. 1, the FV and ROT stations and the FV and ESP stations are ~300 and 400 km apart, respectively. Despite the small difference in remoteness, the co-variability between station temperatures is persistently steady in the first case and is greatly changed over the decades in the second case.

We further analyse the association of the ESP and FV temperature anomalies with the SST anomalies from NNR in winter. The period of high-correlation ESP *vs* FV between 1978 and 2000 (23 years, dashed vertical lines in Fig. 4) is compared with the remaining parts of the time series 2001–17 (17 years), which represents the period of low correlation. The high-correlation ESP *vs* FV is clearly associated with the strong correlation anomalies in the ESP *vs* SST (Fig. 5a) and FV *vs* SST (Fig. 5b) relationships, which exhibit very similar geographical distributions. In both cases, the negative anomalies are concentrated in the central tropical Pacific and the Amundsen Sea region and the positive anomaly is located in the AP–Weddell Sea region.

High-latitude anomalies are known as the Antarctic Dipole pattern, which is a stationary wave structure with an out-of-phase relationship between the Pacific and the Atlantic polar regions, which, in turn, is coupled with the central tropical Pacific (see the Discussion). Note that both anomalies of the Antarctic Dipole are in West Antarctica.

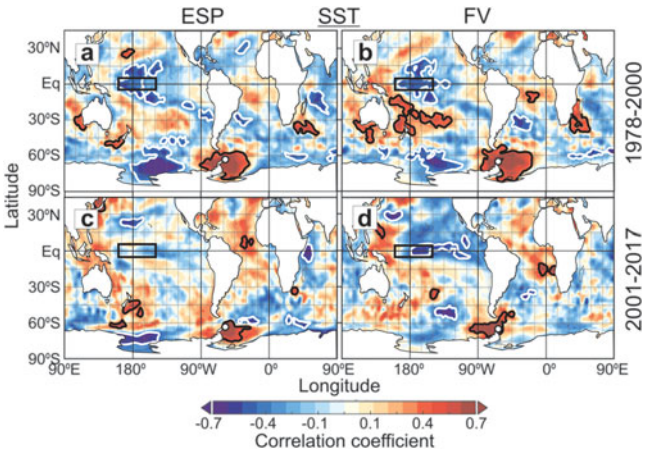

Fig. 5. Correlations between temperature at the Antarctic Peninsula stations **a. & c.** Esperanza (ESP) and **b. & d.** Faraday/Vernadsky (FV) and sea surface temperature from the National Centers for Environmental Prediction (NCEP)–National Center for Atmospheric Research (NCAR) reanalysis for periods of **a. & b.** 1978–2000 and **c. & d.** 2001–17, when high and low correlations of ESP *vs* FV, respectively, were observed (Fig. 4). Winter seasonal averages over June–August are presented. Positive (negative) correlation anomalies significant at the 95% confidence level are outlined by black (white) contours. Rectangle at the equator indicates the Niño-4 region (5°N–5°S, 160–210°E). The circles mark the locations of the stations.

In the recent decades of the 2000s and 2010s, the correlation coefficients are lower and their distributions differ from those in the 1980s and 1990s (lower and upper panels, respectively, in Fig. 5). The warmer ESP (FV) temperature is associated with the warmer eastern (western) AP region as seen from Fig. 5c (Fig. 5d). The ESP temperature remains involved in the Antarctic Dipole variability, including the negative correlation anomaly in the Amundsen–Ross Sea region (~180°E); however, it becomes uncoupled with the tropical Pacific (Fig. 5c). By contrast, the FV temperature retains sensitivity to the tropical SST anomalies extended eastwards along the equator from the central Pacific to the eastern Pacific; however, it loses coupling with the Antarctic Dipole negative anomaly (Fig. 5d).

Decadal changes in the tropical influences on the temperature variations at ESP (NAP) and FV (SAP), which are obvious from Fig. 5c & d, respectively, are accompanied by the changes in the patterns of zonal circulation associated with each of the sub-regions. This is illustrated in Fig. 6 using the correlations between the ESP and FV time series and zonal wind at the 300 hPa pressure level, U300 (9 km, the SH extratropical tropopause level in winter) from the NNR data. The period of high-correlation ESP *vs* FV (Fig. 4) is characterized by the strong meridional wave train between the tropics and the polar SH region (arrows in Fig. 6a & b). The wave pattern in the correlation fields for ESP (Fig. 6a) is very similar to that for FV (Fig. 6b) and also exists at lower altitudes in the troposphere (not shown). It is a manifestation of the pathway of the planetary waves forced by the SST anomalies in the

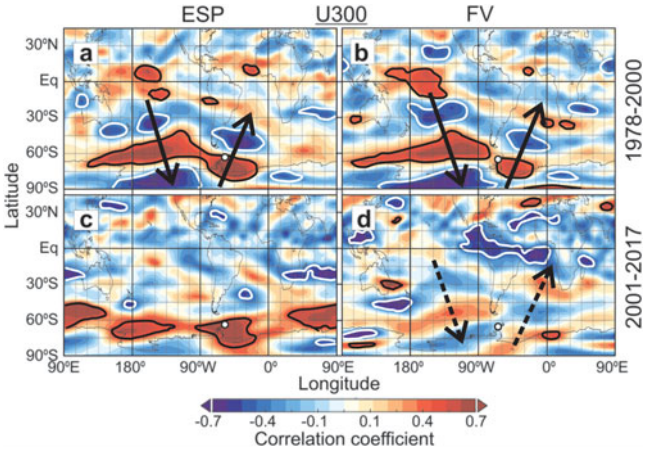

Fig. 6. As in Fig. 5, but for the 300 hPa zonal wind from the National Centers for Environmental Prediction (NCEP)–National Center for Atmospheric Research (NCAR) reanalysis. Arrows indicate the pathway of the meridional wave train of the quasi-stationary planetary waves forced by the tropical sea surface temperature anomalies. ESP = Esperanza, FV = Faraday/Vernadsky.

https://doi.org/10.1017/S0954102020000255 Published online by Cambridge University Press

central tropical Pacific (Fig. 5a & b) and propagated in the SH atmosphere polewards and eastwards (see the Discussion).

Note that the meridional wave train contains the positive and negative correlation anomalies, which are zonally arranged (upper panel in Fig. 6) and are usually attributed to the SAM (see the Introduction). In the AP sector (0–90°W), the negative (positive) anomaly is located north (south) of 60°S (Fig. 6a & b). In the interannual variations, the temperature increase in the AP region in the 1980s and 1990s was accompanied by the zonal wind velocity increase here. In general, the correlation anomalies in Figs 5a & b and 6a & b show that the high-correlation ESP *vs* FV in the 1980s and 1990s (Fig. 4) was due to the strong teleconnection between the central tropical Pacific and the AP region.

Similar teleconnection patterns are observed in correlations with geopotential height at 300 hPa, Z300 calculated using the NNR data (Fig. S4a & b). Note that geopotential height is sensitive to changes in both SLP and the temperature of the layer between the surface and a given pressure level. The negative anomaly in the central tropical Pacific and the positive one over the AP in Fig. S4a & b correspond to the anomalies in correlation with surface temperatures (Fig. 5a & b). Hence, the correlation patterns in Fig. S4a and b indicate a strong negative coupling between the tropics and the AP not only in the surface temperatures (Fig. 5a & b), but also in the tropospheric temperatures below the 300 hPa pressure level. At the same time, the meridional wave train (arrows in Fig. S4a & b) is similar to that in correlation with U300 (Fig. 6a & b).

The teleconnection with the tropics was weakened in 2001–17 (Fig. 6c & d; see also Fig. S4c & d). There are no signs of the wave train pattern in the correlations ESP *vs* U300 and ESP *vs* Z300 (Figs 6c & S4c); however, strong positive correlation anomalies encircle the Antarctic continent. They combine the SAM pattern and the zonal wave 3 pattern. Because of there being three ocean basins separated by continents, the SAM/wave 3 pattern is typical for the SH atmospheric circulation (see the Discussion). The strong positive correlation anomaly over the AP region in Fig. 6c is evidence of the strong dependence of the ESP temperature on the zonal wind at the interannual timescale. Correlation with the surface zonal wind shows a similar positive anomaly just above the northern peninsula (Fig. 7a).

A statistically insignificant wave train pattern is seen in the correlation FV *vs* U300 (dashed arrows in Fig. 6d; see also Fig. S4d). Near-zero anomaly at FV is seen in correlation with the surface zonal wind (Fig. 7b), and both stations are located on the edge of the significant negative anomaly in correlation with the meridional surface wind (Fig. 7c & d).

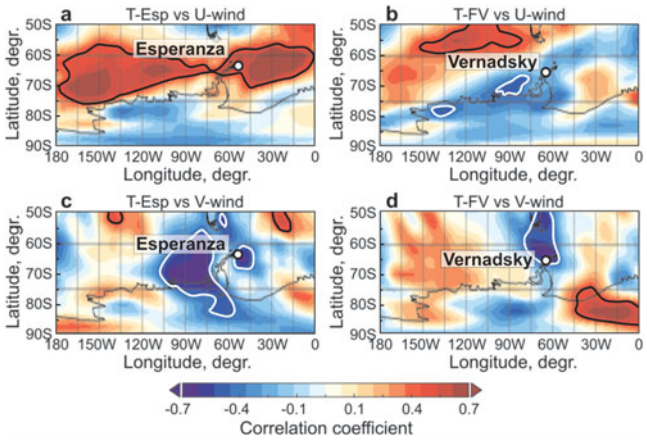

Fig. 7. Correlation between **a. & b.** surface zonal wind and **c. & d.** surface meridional wind from the National Centers for Environmental Prediction (NCEP)–National Center for Atmospheric Research (NCAR) reanalysis data and observed temperature at **a. & c.** Esperanza (ESP) and **b. & d.** Faraday/Vernadsky (FV). The period 2001–17 and the western hemisphere between 50°S and 90°S are shown.

The results in Figs 4–7 and S4 show that a high coherence in the SAP and NAP temperatures exists in the period of the strong tropical teleconnection (1980s–1990s). Since the 2000s, when NAP and SAP temperatures correlate insignificantly, the effects of tropical forcing are greatly weakened. The SAM/wave 3 pattern dominates the correlation with ESP and warming continues in the NAP, while there are no noticeable manifestations of climate modes in correlation with FV, and the SAP is in a condition of cooling (or absence of warming).

Surface wind variability

We have examined variability in wind direction and wind speed in the NAP (time series for ESP) and SAP (time series for FV and ROT) using the READER data (Fig. 8). Wind directions are mostly westerly and northerly at ESP and ROT, respectively (Fig. 8a & c), and are very variable at FV with predominating northerly (near 0°E) and easterly (0–180°E) winds (Fig. 8b).

The high variability in the wind direction at FV is explained by local orography, with the island landscape around the station and the AP mountains to the east serving as barriers to the zonal circulation (Fig. 2). In addition, mean wind speed at FV (4.6 ms^{-1}; Fig. 8e) is approximately two times slower than at ESP (8.4 ms^{-1}; Fig. 8d) and 1.5 times slower than at ROT (6.5 ms^{-1}; Fig. 8f); therefore, the FV wind direction may undergo greater variability (Fig. 8b). This is why we illustrate wind variability using the monthly means from the READER data for June, July and August (black, red and blue symbols, respectively, in Fig. 8). A simple

https://doi.org/10.1017/S0954102020000255 Published online by Cambridge University Press

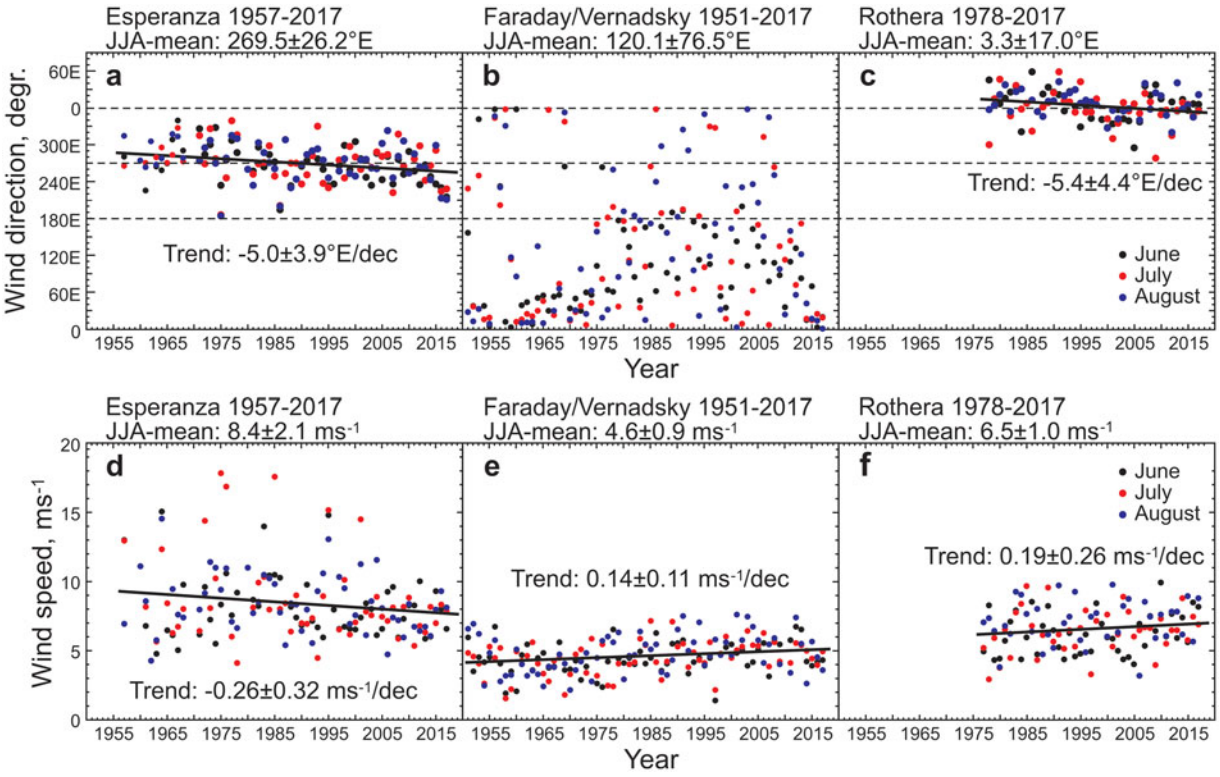

Fig. 8. Interannual variability of **a.–c.** wind direction and **d.–f.** wind speed at **a. & d.** Esperanza, **b. & e.** Faraday/Vernadsky and **c. & f.** Rothera from the Reference Antarctic Data for Environmental Research (READER) data. Black, red and blue symbols are for the winter months June, July and August (JJA), respectively. Solid lines are the linear trends of the JJA means. The trend values with the 95% confidence limits and means with ± 1 standard deviation are indicated.

averaging over June–August of the wind directions, which are close, for example, to 360°E and 0°E and contain mostly northerly wind components, would give the value of ~180°E; that is, southerly wind. A more correct approach is calculation of the zonal and meridional wind components using wind speed and wind direction starting from the daily measurements. These calculations require more work and are planned for a future study. Based on the close correlations between temperatures from observations and reanalyses ($r = 0.8–0.9$; Fig. S2), we use the reanalysis data for the zonal and meridional wind components below.

The wind at ESP steadily moved in the direction from west–north-west to west–south-west with a slow rate of -5.0 ± 3.9°E decade^{-1} (significant at the 95% confidence level; solid line in Fig. 8a). At ROT, a shift from north–north-east to north–north-west occurred with a similar slow rate of -5.4 ± 4.4°E decade^{-1} (solid line in Fig. 8c).

Decadal variability with respect to linear tendency is especially important for the temperature changes in the SAP. Here, the turning towards north–north-east winds (blowing from the sector 0–90°E; i.e. from the AP ice sheet; see Fig. 2) that occurred at FV and ROT in recent decades (Fig. 8b & c) was favourable for the relative cooling there. Note that the coldest period of 1950s–1970s at FV (Fig. 3a) was characterized by the same wind conditions (Fig. 8b). As shown below, the development of a SLP anomaly close to the AP region may influence local changes in wind direction and speed.

The dependence of the temperature changes on the wind directions in the NAP and SAP is presented in Figs 9 & 10 using linear regression. We have compared observed temperature variabilities in the NAP (ESP time series) and SAP (FV time series) *vs* zonal and meridional wind component variability taken from the NNR surface wind data and ERA 10 m wind data. The wind components have been extracted from the reanalysis grid points, which are the closest to the station coordinates (see caption for Table SII). Both reanalyses are consistent in the regression tendencies and statistical significances of the regression coefficient B, although there are differences in the regression coefficient values (Figs 9 & 10).

The B slopes of the regression lines demonstrate that long-term and recent temperature variabilities at ESP are associated with the westerly wind component U (Fig. 9a & c), which transports warmer air from the west. As is seen from Fig. 8a, west–north-west and west–south-west wind components at ~270°E may contribute to warming at ESP (Fig. 3d). The statistical significance of the

https://doi.org/10.1017/S0954102020000255 Published online by Cambridge University Press

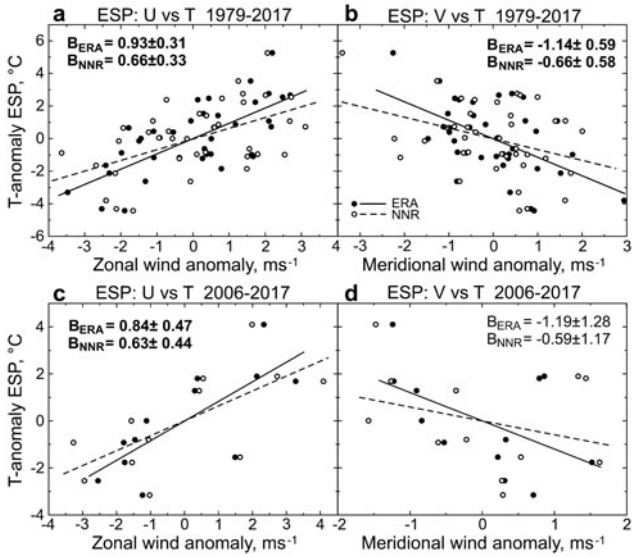

Fig. 9. Linear regression between the de-trended time series of the Esperanza (ESP) surface temperature and zonal and meridional wind components in **a. & b.** 1979–2017 and **c. & d.** 2006–17. Positive zonal (meridional) wind speed anomaly is for the westerly (southerly) wind component. Wind components from ERA Interim (ERA; closed circles and solid regression lines) and National Centers for Environmental Prediction (NCEP)–National Center for Atmospheric Research (NCAR) reanalysis (NNR; open circles and dashed regression lines) are taken at the grid points closest to the station locations (Table SII). The B slopes of the regression lines significant at the 95% confidence level are indicated in bold.

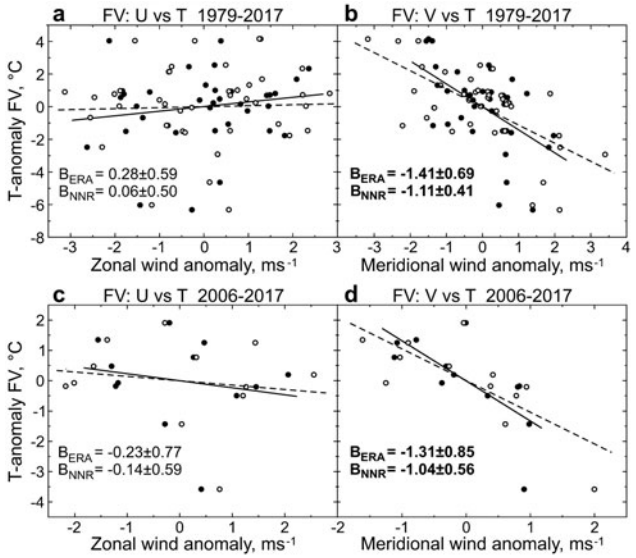

Fig. 10. As in Fig. 9, but for the Faraday/Vernadsky (FV) surface temperature. ERA = ERA Interim, NNR = National Centers for Environmental Prediction (NCEP)–National Center for Atmospheric Research (NCAR) reanalysis.

U–T coupling at ESP in 2006–17 is at the 95% confidence limit in terms of both regression (Fig. 9c) and correlation ($r = 0.67$ for NNR and $r = 0.75$ for ERA; Table SII). The V–T coupling is statistically significant at the 90% confidence limit in terms of regression (Fig. 9d) and insignificant in terms of correlation ($r = -0.30$ for NNR and $r = -0.51$ for ERA; Table SII).

The positive, although not statistically significant, trends in the U component at ESP are present in the reanalysis data for the 2006–17 period (Table SIII). As a result, the ESP temperature warming in 2006–17 consists of 31% (67%) of the temperature trend congruent with the U trend in the NNR (ERA) time series; however, this trend component is statistically insignificant (Table III).

Unlike ESP, the meridional (zonal) wind component is a determining (insignificant) factor in the FV temperature variability, as is seen from Fig. 10b & d (Fig. 10a & c). This is in agreement with the correlation anomalies in the FV area in Fig. 7d (Fig. 7b) and the correlation coefficients in Table SII. The regression coefficients for V *vs* T are statistically significant in terms of both long-term temperature change (Fig. 10b) and recent cooling (Fig. 10d). The regression line slopes presented in Fig. 10d become less steep if the anomaly of -10°C in the observed FV temperature in 2015 (Fig. 3a) is excluded ($B = -0.89 \pm 0.60$ and $B = -0.63 \pm 0.58$ for ERA and NNR, respectively) and remain statistically significant at the 95% confidence limit (not shown).

Winter cooling at FV in 2006–17 resulted partly from northerly wind weakening (statistically insignificant; Table SIII). The V-congruent component of the FV temperature decrease in 2006–17 is 37% (21%) from the NNR (ERA) time series (Table III) and is statistically insignificant. Note that westerly winds at FV were observed more frequently in the 1980s and 1990s (0–180°W; Fig. 8b) in the period of rapid warming (Fig. 3a), whereas they ceased in recent decades (Fig. 8b), favouring a cooling tendency (Fig. 3a).

On the whole, Figs 9 & 10, as well as Tables III, SII and SIII, show that the recent change in surface temperature along the AP was to some degree a response to changes in zonal and meridional winds, namely the NAP warming contributed by the westerly wind enhancement, whereas the SAP cooling was partly due to the northerly wind weakening.

Climate mode effects

The results in Figs 5–7, 9 & 10 indicate that consistent or inconsistent winter temperature variations between the NAP and SAP are, to a large extent, dependent on the interaction between the remote (tropical temperature anomalies) and local (zonal and meridional circulation

https://doi.org/10.1017/S0954102020000255 Published online by Cambridge University Press

Table III. The part of the station temperature trends (%) contributed by zonal (U) and meridional (V) wind components and by Southern Annular Mode and Niño-4 climate indices in 2006–17 as estimated by the method of congruent trend.

	Congruent with	Percentage	Statistical significance
Esperanza	U-NNR	31%	Statistically insignificant
	U-ERA	67%	Statistically insignificant
Faraday/ Vernadsky	V-NNR	37%	Statistically insignificant
	V-ERA	21%	Statistically insignificant
Esperanza	SAM	75%	Statistically significant at 70% confidence limit
Faraday/ Vernadsky	N4	59%	Statistically significant at 85% confidence limit

ERA = ERA Interim, NNR = National Centers for Environmental Prediction (NCEP)–National Center for Atmospheric Research (NCAR) reanalysis.

anomalies) influences. As noted in the Introduction, the interaction between the main modes of climate variability influences AP climate change on decadal timescale. To estimate quantitatively decadal changes in such an interaction, we have calculated the running correlation between the ESP and FV time series and the indices for the N4 region and SAM and AAO, described above. The N4 region is located in the central tropical Pacific (rectangle at the equator near 180°E in Fig. 5), where the SST anomalies are strongly negatively correlated with the ESP and FV temperatures (Fig. 5). The running correlations in Fig. 11 show notable decadal variability in the strength and significance of coupling between the NAP and SAP station temperature and climate indices.

The N4 index shows persistent negative correlations (significant at the 95% confidence limit) with the station data during the 1980s and 1990s (Fig. 11a). Correlation with FV (dashed curve) is consistently stronger than with ESP (solid curve), indicating stronger tropical influence on the SAP than on the NAP. This difference corresponds to a larger correlation anomaly in the N4 region for FV than for ESP (compare filling with the negative *r*-values of the rectangle at the equator in Fig. 5b & a, respectively). Decadal tendencies in Fig. 11a are similar to those in Fig. 4, particularly with respect to persistently strong correlations during the 1980s and 1990s. This coincidence indicates that the dominant factor of the co-variability in the temperatures along the whole AP is the intense wave train (Fig. 6a & b) forced by the strong SST anomalies in the central tropical Pacific (Fig. 5a & b).

Weakened tropical teleconnection in the last decade (Fig. 6c & d) has various effects on the NAP and SAP, as seen from the end portions of the curves in Fig. 11a: the solid curve for ESP is here at the level of $r \approx -0.3$, which is non-significant statistically, while the dashed curve for FV reaches 95% significance at $r \approx -0.6$. This confirms a closer connection of the N4 region with the SAP than with the NAP noted above. Student's *t*-tests show that the N4 trend in 2006–17 (Fig. S3b) is significant at the 85% confidence level. Then, based on the regression 'N4 *vs* FV temperature' (Fig. S5d), the FV temperature decrease in 2006–17 consists of 59% of the N4-congruent trend (Table III) at the same 85% significance level.

The Annular Mode indices are less persistent in their coupling with the station temperatures in comparison with the N4 index. This can be seen from Fig. 11b & c, where the relatively short-term peaks of the positive correlation appear in different decades for ESP and FV. During the 2000s–2010s, the ESP temperature shows the strongest positive correlations at $r = 0.8$–0.9 with SAM and AAO (solid curves in Fig. 11b & c), in agreement with the results for zonal wind in Figs 6c & 7a. Another significant peak in the correlation ESP *vs* AAO is seen in the 1980s; however, it is non-significant statistically in the correlation ESP *vs* SAM. We believe that the AAO index is preferable to the SAM index for the AP region because the high-latitude data used for the SAM index are based mainly on the stations of East Antarctica (see further argument in the Discussion). The FV temperature response to the Annular Mode variability is weaker than that of ESP (dashed and solid curves, respectively, in Fig. 11b & c). The single period of the stable coupling for FV *vs* SAM/AAO is the 1990s (dashed curves in Fig. 11b & c).

Interestingly, the correlation peaks in the 1980s (solid curves for ESP in Fig. 11b & c) and the 1990s (dashed curves for FV in Fig. 11b & c) are also observed in the correlation ESP *vs* FV (Fig. 4). Hence, co-variability between the ESP and FV temperatures in the 1980s and 1990s (Fig. 4) displays the individual sensitivity of the stations to the Annular Mode; however, this occurs only in the period of the strong tropical influences (Fig. 11a). Later, weakened tropical teleconnection (Fig. 11a) is associated with uncoupled temperature variations between the NAP and SAP (Fig. 4), and the Annular Mode influence dominates in the NAP after 2000 (solid curves in Fig. 11b & c), which is in agreement with the results of Figs 5–7.

Note that the average correlations between the SST anomalies in the tropics and Annular Mode are very low: $r = 0.11$ for N4 *vs* SAM (1957–2017) and $r = -0.11$ for N4 *vs* AAO (1979–2017). The running correlation N4 *vs* SAM (Fig. S6a) varies in the range $r = \pm 0.4$ (which is non-significant statistically). This means that the two climate modes are almost uncoupled even in the period of their concurrent impacts on the AP.

In the last period 2006–17, high-correlation SAM *vs* ESP ($r = 0.7$–0.9; Fig. 11b) is accompanied by a high

https://doi.org/10.1017/S0954102020000255 Published online by Cambridge University Press

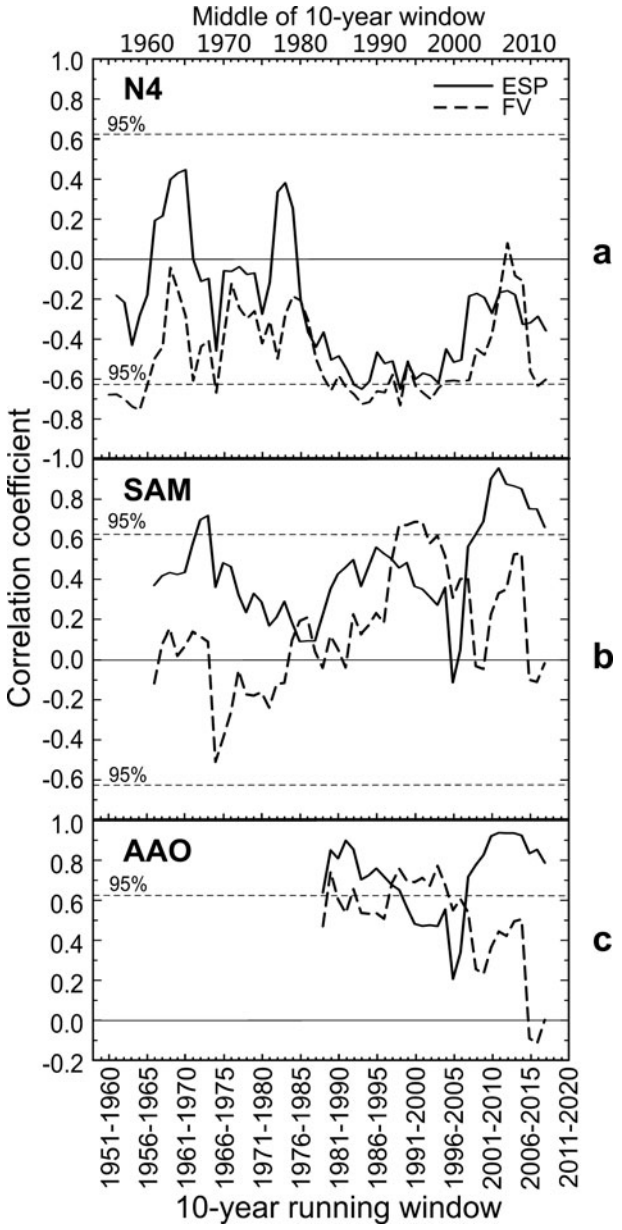

Fig. 11. Running correlation with a 10 year window between the winter temperature at Esperanza (ESP) and Faraday/Vernadsky (FV) and the climate indices **a.** Niño-4 (N4), **b.** Southern Annular Mode (SAM) and **c.** Antarctic Oscillation (AAO).

positive SAM trend (1.11 ± 2.03, significant at the 70% confidence level; Fig. S3a). Along with significant linear regression SAM *vs* ESP (1.37 ± 0.80, significant at the 99% confidence level; Fig. S5a) in the same period, this provides convincing evidence that the positive SAM trend contributed to the ESP (and NAP) warming in 2006–17. The SAM-congruent component in the positive temperature trend at ESP in 2006–17 is 75% (significant at 70% confidence level; Table III).

Generally, winter warming in West Antarctica was also contributed by increasing SST in the central Pacific through the teleconnection mechanism (see the Introduction). Despite the positive N4 trend in 2006–17 (Fig. S3b), the insignificant correlation for ESP *vs* N4 (Fig. 11a, solid curve) and the regression N4 *vs* ESP being significant at the 80% confidence level (-1.81 ± 2.74; Fig. S5b) indicate that the two time series are almost uncoupled. This excludes the noticeable tropical teleconnection effect in the NAP warming from the N4 region (Fig. 5c).

The SAM/N4 interannual variability in our results indicates occasional concurrent contributions to the AP surface temperature variability in the winter only in the 1980s and 1990s (e.g. FV *vs* N4: $r = -0.63$ and FV *vs* SAM: $r = 0.69$ in the window 1991–2000; dashed curves in Fig. 11a & b, respectively), when both indices show an increasing trend (Fig. S3). Low correlations between FV and the SAM and N4 indices dominate since *c.* 2000 (dashed curves in Fig. 11). The correlation FV *vs* N4 reaches the 95% confidence limit at $r = 0.62$ only in the 10 year window from 2007 to 2016 (dashed curve in Fig. 11a). Note that anomalously high SST in the N4 region in 2015 (29.8°C; Fig. S3b) was associated with the lowest temperature at FV in 2006–17 (-10°C; Fig. 3a). This correspondence supports general negative coupling between the N4 and SAP temperatures. The negative correlation anomaly partially falls into the N4 region (Fig. 5d); therefore, this region partially contributed to the SAP temperature change in correspondence with the N4-congruent trend at FV (59%; Table III).

As the large-scale patterns of the climate modes (meridional wave train from the tropics and zonal SAM structure) are not present in Fig. 6d, these modes are not significant contributing factors to the recent FV temperature change, suggesting a dominance of the local/regional circulation effects.

In order to clarify the possible relationship between the large-scale and local processes suggested by the SAM–N4 coupling, we have analysed decadal tendency in the SLP anomalies in the SH using NCEP–NCAR reanalysis data (Fig. 12). The SLP anomalies with respect to the 1981–2010 climatology display decadal change in the SAM phase. The dotted line in Fig. S3a shows that the SAM trend in winter in the last six decades (0.17 ± 0.17° decade^{-1}) was towards a positive phase (in agreement with the known tendency, see the Introduction) and was significant at the 95% confidence level. The prevailing negative SAM phase in the 1950s–1970s (Fig. S3a) corresponds to a strong anomaly in the high SLP, which is almost uniformly distributed around the Antarctic continent (Fig. 12a).

By contrast, a shift to the positive SAM phase in the 2000s–2010s (Fig. S3a) is accompanied by a negative SLP anomaly, which is localized to the west of the

https://doi.org/10.1017/S0954102020000255 Published online by Cambridge University Press

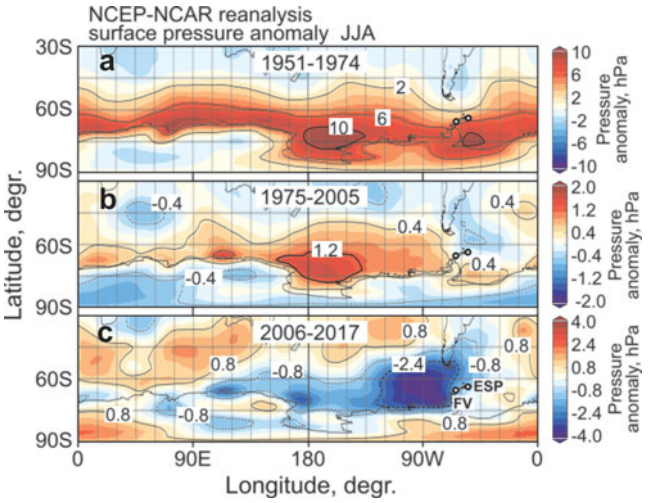

Fig. 12. Sea-level pressure anomalies south to 30°S in **a.** 1951–74, **b.** 1975–2005 and **c.** 2006–17 with respect to the 1981–2010 climatology. Data taken from National Centers for Environmental Prediction (NCEP)–National Center for Atmospheric Research (NCAR) reanalysis. JJA = June, July and August.

AP (Fig. 12c). The negative peak of -4 hPa is located in the Bellingshausen Sea at ~90°W. In recent decades, this SLP anomaly adjacent to the AP from the west could be an important factor affecting the AP temperature changes. Its action is possible through the changes in both coupling between SAM and N4 and in the local circulation in the AP region, including the relationships between the zonal and meridional winds in the NAP and SAP described above. Note that the sharp SLP gradient is closer to the SAP than to the NAP (Fig. 12c).

Summarizing the results of this subsection, we can conclude that: 1) enhanced SAM/N4 influences in the 1980s and 1990s produced the warming effects in SAP and NAP, 2) SAM contributed to the NAP warming and N4 partially contributed to the SAP cooling in the 2000s and 2010s, and 3) the negative SLP anomaly to the west of the AP in recent decades could introduce changes in the relationships between the zonal and meridional winds on the NAP and SAP temperatures.

Discussion

Differences between the AP sub-regions

We have analysed the difference in the decadal change of the winter temperature between the NAP and SAP. This approach was motivated by the obvious difference in the temperature trends of warming and cooling, respectively, in the last decade (Fig. 1b). Such difference contrasts with a general warming tendency over the peninsula during the preceding five decades (Figs 1a, 3 & S1, upper panel), which is well known from many works (King 1994, Vaughan *et al.* 2003, Turner *et al.* 2005, Ding & Steig 2013, Tymofeyev 2014, Clem *et al.* 2016). As is seen from Fig. S1 (upper panel), persistent warming over the entire AP in 1951–2005 occurred in each season, while the recent cooling in the annual mean temperature (Fig. S1j) was mainly due to spring and summer negative trends (Fig. S1g & h). This is generally consistent with previous studies (Carrasco 2013, Turner *et al.* 2016, Oliva *et al.* 2017). With seasonal variability of cooling and warming over the AP in 2006–17 (Fig. S1f–i), opposite tendencies in the two AP sub-regions are observed only in winter (Fig. 1b, reproduced in Fig. S1f for ease of comparison).

We noted that the correlations decrease with increasing AP station separation (King 1994, Kravchenko *et al.* 2011, Oliva *et al.* 2017, Turner *et al.* 2019), and we illustrated this tendency in Fig. 3 and Table I. On average for 1952–2017, the correlation ESP *vs* FV is statistically significant with $r = 0.56$ (at the 99% confidence level; Table I); however, as is seen from Fig. 4, this correlation varies on decadal timescale between $r = 0.2$–0.3 and $r = 0.6$–0.9. This indicates that, under conditions of large spatial variability in the AP temperature (King 1994, King & Comiso 2003, van Wessem *et al.* 2015, Turner *et al.* 2019), periods of both low and high coherency in the interannual temperature variations over the NAP and SAP exist.

From our results, the two important factors that characterize the similarity and difference between the decadal temperature changes in the NAP and SAP can be emphasized. First, the winter temperatures observed at the NAP and SAP stations are strongly correlated only in the period of the 1980s and 1990s (Fig. 4). In this period, high correlations between the observed AP temperatures and the climate indices N4 and SAM (Fig. 11), in combination with increasing trends in both indices (Fig. S3), favour the temperature co-variability in the NAP and SAP (Fig. 4), with consistent warming over the entire AP region (Figs 3 & 13a).

Second, the temperature correlation between the NAP and SAP stations in recent decades (the 2000s and 2010s) is low (Fig. 4), and the temperature trends here become opposite, especially in 2006–17 (Figs 1b & 3). If the SAM effect with a warming tendency continued to dominate the NAP region (Figs 6c, 11b & c & S5a), the weakened SAM/N4 influences (Figs 11, S5c & d & S6b) resulted in the relative SAP cooling in this period (Fig. 3a & b). There were different levels of the influence of SAM and N4 on the northern and southern parts of the AP, despite there being positive trends in both modes (Fig. S3). These differences were accompanied by changes in the local zonal and meridional wind components (Figs 9 & 10), which in turn seem to be associated with the development of the negative regional SLP anomaly to the west of the AP (Fig. 12).

https://doi.org/10.1017/S0954102020000255 Published online by Cambridge University Press

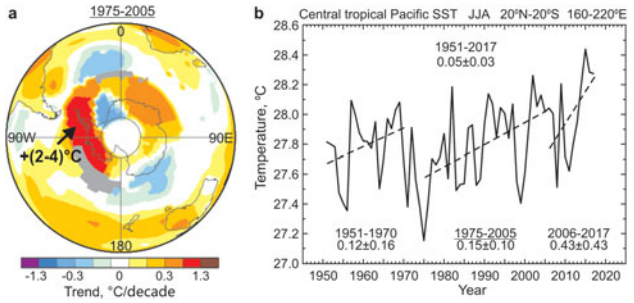

Fig. 13. a. Decadal trend of the Southern Hemisphere sea surface temperature (SST) in winter 1975–2005, the period of the strongly correlated temperatures at Esperanza (northern Antarctic Peninsula) and Faraday/Vernadsky (southern Antarctic Peninsula). The arrow indicates the total temperature increase over a 31 year period. The NASA Goddard Institute for Space Science data are used. Compare with Fig. 1a. **b.** Time series of the central tropical Pacific SST in June, July and August (JJA) 1951–2017 averaged over 20°N–20°S, 160–220°E. From the National Centers for Environmental Prediction (NCEP)–National Center for Atmospheric Research (NCAR) reanalysis data. Piecewise linear trends (dashed lines) are indicated with their 95% confidence limits.

A similar north–south AP division with positive (negative) surface temperature anomalies in the NAP (SAP) is associated with positive anomalies in the indices for SAM and teleconnection with the central tropical Pacific (Marshall & Thompson 2016, their fig. 3b & d). According to Marshall & Thompson (2016), positive SAM polarity causes a warmer NAP and a colder SAP and rest of Antarctica in all seasons. It is known that the enhancement of zonal circulation associated with positive SAM contributes to increased advection of warm air masses towards the AP and reduced polewards advection of heat with cooling over Antarctica (Thompson & Solomon 2002, Marshall *et al.* 2006). A boundary between those regions of Antarctica where temperatures are positively and negatively correlated with the SAM exists, and the line that separates these regions moves through the latitude of FV twice a year (Marshall 2007). In our results, the recent north–south division in the AP temperature change occurred only in winter (Figs 1b & S1f–i) and, as noted above, combines three possible sources: positive SAM trend, weakened tropical teleconnection and deepening negative SLP anomaly.

The N4 and Annular Mode impacts

The atmospheric circulation in the SH is mainly determined by the El Niño–Southern Oscillation (ENSO) and SAM influences, and their interaction strongly affects the AP climate (Kwok & Comiso 2002, Schneider *et al.* 2012, Yu *et al.* 2012, Clem & Fogt 2013, Clem *et al.* 2016, Marshall & Thompson 2016, Yuan *et al.* 2018). Warming of West Antarctica is associated with tropical influences due to increasing SST in the central Pacific and teleconnection (Ding *et al.* 2011, Schneider *et al.* 2012, Clem & Fogt 2013). On the other hand, the general long-term trend towards the positive phase of the SAM index over the past half-century produces a spatial pattern with warmer temperatures in the AP (Kwok & Comiso 2002, Marshall 2003, 2007, Fogt & Bromwich 2006, Marshall *et al.* 2006, Marshall & Thompson 2016). The close relationship between the climate modes, temperatures, winds and sea-ice cover in the AP region was noted (Marshall 2007, Stammerjohn *et al.* 2008a, 2008b, van Wessem *et al.* 2015).

Our results indicate that the period of the 1980s and 1990s of the high-correlation ESP *vs* FV is characterized by the joint action of both phenomena over the AP region (Fig. 11). The ENSO effect appears due to the SST anomalies in the central tropical Pacific (the N4 region), which are strongly negatively correlated with the ESP and FV temperatures (Fig. 5a & b). The SST increase in the N4 region (Figs 13b & S3b) contributed to AP warming through teleconnection (Fig. 6a & b). It should be emphasized that decadal temperature trends in the 1980s–1990s were consistently positive in regions of the N4 (Figs 13 & S3b) and AP (Fig. 3), but they occurred with a strong negative correlation between these remote regions on the interannual timescale (Figs 5a & b & Fig. 11a).

The decadal SAM trend (Fig. S3a) also contributed to the AP warming in the 1980s and 1990s, but with a greater decadal variability than N4 (Fig. 11b & c). The Annular Mode influence reached maxima in the 1980s and since 2000 in a case of the ESP temperature (solid curves in Fig. 11b & c) and only in the 1990s in a case of the FV temperature (dashed curves in Fig. 11b & c). Using the 20 year running window, Marshall (2007) has shown that a significant positive correlation for SAM *vs* ESP was observed in winter between 1981–2000 and 1985–2004 (his fig. 4c), which, in general, is consistent with Fig. 11b & c (solid curves).

The results of Fig. 11 show that the SAM/AAO-related decadal changes in the winter temperature may be independent in the NAP and SAP; additionally, they can develop independently of the N4-related changes. The SAM and N4 indices appear to be almost uncoupled, as is seen from the low running correlation at $r = \pm 0.4$ (not significant at the 90% confidence level; Fig. S6a) and low average correlation $r = 0.1$. This is consistent with Kwok & Comiso (2002), who analysed the same two decades (between about 1980 and 2000); it was noted that regional winter warming of the AP in this period could be associated with possible interactions of the modes of atmospheric variability described by the SAM and Southern Oscillation indices, which are uncorrelated.

https://doi.org/10.1017/S0954102020000255 Published online by Cambridge University Press

As is shown for spring (September–November), the two decades of the 1980s and 1990s may differ in the strength of the ENSO teleconnection to the AP region due to the out-of-phase (in-phase) relationship between ENSO and SAM in the 1980s (1990s) (Fogt & Bromwich 2006, Stammerjohn *et al.* 2008a, 2008b, Yu *et al.* 2015). According to Stammerjohn *et al.* (2008a), the Niño-3.4 and SAM indices show significant negative correlation in spring over 1992–2004, with $r = -0.60$. Hence, the SAM–ENSO coupling is variable on the decadal timescale and is seasonally dependent.

Clem & Fogt (2013) used the 10 year running correlations between the AP temperatures and the Southern Oscillation index (SOI) and SAM index. They have shown that the SOI influence is persistent at the SAP stations (Faraday and ROT) and the SAM influence is persistent at the NAP stations (ESP and MAR) over the full period of record at each station. Our results for winter do not demonstrate long-term persistence in similar correlations, especially with respect to SAM/AAO (Fig. 11).

The relatively steady N4 signal in the AP temperature observed during the 1980s and 1990s (Fig. 11a) should be almost identical to the SOI effects, as El Niño and Southern Oscillation relate to the same phenomenon, which is described by the oceanic and atmospheric anomaly index, respectively (www.wmo.int/pages/prog/wcp/wcasp/documents/JN142122_WMO1145_EN_web.pdf). Correlations between N4 and SOI in 1952–2017 are high ($r = -0.75$ for the winter months and $r = -0.90$ for the spring months), which means there is an almost identical description of the tropical anomaly variability by the two indices. Hence, persistent SOI effects in spring in Clem & Fogt (2013) and variable N4 effects in winter in our results (Fig. 11a) could be manifestations of the seasonal tendencies in the interaction between the tropics and the AP region, which deserve separate analysis.

Note that the correlations with the AAO index (Fig. 11c) are on average higher than with the SAM index (Fig. 11b), especially in the 1980s. The SAM index is based on the station data; however, the selected Antarctic stations are located mainly at the eastern continent boundary (Marshall 2003). Therefore, the climate variability in West Antarctica (Figs 5 & 6) could be relatively more weakly reflected in the SAM index, considering that the Pacific component of the SAM is influenced by wave train that emanated from the tropical Pacific (Ding *et al.* 2012). The AAO index is based on reanalysis data (Mo 2000) and equally represents anomalies at different longitudes. This is why the correlations with the AP station temperatures can reveal a stronger coupling with the AAO index (Fig. 11c) than with the SAM index (Fig. 11b).

It is important to emphasize that the strong tropical teleconnection (upper panels in Figs 5 & 6 and both curves in Fig. 11a) and resulting high-correlation ESP *vs* FV (Fig. 4) are limited to the period 1980s and 1990s. Taking into account the full size of the 10 year window in the running correlation, the strong teleconnection period can be considered to have lasted over three decades, approximately during 1975–2005. This is the period of the most rapid warming in the AP region, with the trends of 1.77° decade^{-1} (FV) and 0.54° decade^{-1} (ESP), which are significant and non-significant at the 95% confidence level, respectively (compare with the trends in Table II: 1.05° decade^{-1} and 0.32° decade^{-1}, respectively). This period gives the main contribution to AP warming since 1951. As is seen from Fig. 13a, the largest warming of 2–4°C in 1975–2005 is concentrated in West Antarctica, including the AP. Substantial winter warming in the close 31 year period of 1979–2009 was noted over the entire West Antarctica (Ding *et al.* 2011) and was also associated with the wave train forced by the SST anomalies in the central tropical Pacific.

The decadal SST increase in the tropical region suggests strengthened anomalous deep convection and intensified wave train forcing (Ding *et al.* 2011, Schneider *et al.* 2012, Ding & Steig 2013). Figure 13b demonstrates a steady warming tendency in the central tropical Pacific (20°N–20°S, 160–220°E) over 1951–2017 with a linear trend of 0.05 ± 0.03°C decade^{-1} significant at the 95% confidence level. In the period of strong teleconnection of 1975–2005 (Figs 5a & b & 6a & b), warming throughout the entire AP (Figs 3 & 13a) is consistent with the positive SST trend of 0.15 ± 0.10°C decade^{-1} in the central tropical Pacific region (dashed line for 1975–2005 in Fig. 13b) and of 0.22 ± 0.21°C decade^{-1} in the N4 region (dashed line for the same period in Fig. S3b). Note that SST warming also occurred outside this period (piecewise trends for 1951–1970 and 2006–17 in Figs 13b & S3b). However, because of the absence of stable teleconnection (Figs 6c & d & 11a), tropical warming is not associated with AP warming in those periods.

After *c.* 2000, the weakened correlation ESP *vs* FV (Fig. 4) is accompanied not only by a weakened tropical influence (Fig. 11a), but also by a significant distinction in the Annular Mode effects between the NAP and SAP (Fig. 11b & c). Annular Mode action is strong in the northern peninsula (Figs 6c, 7a & S4c and solid curves in Fig. 11b & c), which seems to be a contributing factor to the warming tendency prevailing here since *c.* 2006 (Figs 1b, 3c–e & S5a). The SAM-congruent temperature trend at ESP in 2006–17 is 75% (significant at a 70% confidence level; Table III). Note that the correlations temperature *vs* U300/Z300 for ESP show the prevailing SAM pattern with a positive anomaly at the AP together with a wave 3 element (Figs 6c & S4c). The quasi-stationary wave 3 variations in the SH extratropics are associated with regional changes from meridional to

https://doi.org/10.1017/S0954102020000255 Published online by Cambridge University Press

zonal flow or vice versa (Raphael 2004). The zonal wind anomalies related to wave 3 dominate the NAP climate in 2006–17 (Figs 6c & 7a).

The cooling tendency in the SAP (Figs 1b & 3a & b) is coincident with the weakening impact from the Annular Mode (dashed curves in Figs 11b & c & S5c) and partial contribution from the tropics (dashed curve in Figs 11a & S5d). The latter confirmed the N4-congruent component in the FV temperature decrease in 2006–17 (59%, significant at the 85% confidence level; Table III). Note that the start of the AP cooling throughout the year had been detected since the late 1990s by Turner *et al.* (2016), who concluded that local factors played a greater role than tropical variability. Our results indicate that the tropical impact is partially present in the SAP cooling in winter 2006–17. The specific relationship between strength of Annular Mode and tropical influences in winter 2006–17 provides opposite climate tendencies in the NAP and SAP, suggesting that the boundary between warming and cooling crosses the AP (Marshall 2007, Marshall & Thompson 2016).

The role of negative SLP anomaly

A negative anomaly in the Amundsen Sea region that is also seen in the correlation N4 *vs* SST (Fig. 5a & b) is an element of the Antarctic Dipole (Yuan & Martinson 2001). It is located in a region of strong anomaly in the surface pressure named the Amundsen Sea Low (ASL) (Turner *et al.* 2013) or Amundsen–Bellingshausen Sea Low (Fogt *et al.* 2012). The ASL is the climatological low-pressure anomaly over the latitude band 60–70°S, which comprises the Ross Sea, the Amundsen Sea and the Bellingshausen Sea (Raphael *et al.* 2016). Being the elements of the same wave train (Fig. 6a & b), negative and positive correlation anomalies in the ASL and AP regions, respectively, are manifestations of the central tropical Pacific teleconnection. This is consistent with the well-known fact that the dipole pattern in West Antarctica is closely tied to variability in ENSO and a tropically forced wave train (Yuan & Li 2008, Turner *et al.* 2013, Clem *et al.* 2017).

The negative SLP anomaly that appeared recently in the ASL region (Fig. 12c) was noted in Clem & Fogt (2013), Turner *et al.* (2016, 2019) and Clem *et al.* (2017) as one of the possible climate-forming factors in the AP region. The ASL depth is dependent on the tropical teleconnection, as is mentioned above, and is strongly influenced by the SAM phase with negative SLP anomalies when the SAM is positive (Fogt *et al.* 2012, Turner *et al.* 2013, 2019, Clem *et al.* 2017). Note that the negative SLP anomaly in Fig. 12c is centred at ~90°W in the Bellingshausen Sea region. Unlike this, the ASL in winter locates typically in the Amundsen Sea region at mean longitudes of 130–150°W (Fogt *et al.* 2012, their fig. 3d–f; Turner *et al.* 2013, their fig. 4a). The recent SLP anomaly in the Bellingshausen Sea region (Fig. 12c) occupies the easternmost longitudes among any possible east–west positions that are observed in the year-to-year variations of the ASL in winter (Fogt *et al.* 2012). In general, it is unusual for the ASL to be located so far east in winter.

Describing above the negative SLP anomaly (Fig. 12c), we noted that the sharp SLP gradient is closer to the SAP than to the NAP. As was found by Turner *et al.* (2019, their fig. 2c & d), there is a significant (insignificant) negative correlation between mean SLP in the area of the ASL and Vernadsky (ESP) annual mean temperature. The authors conclude that the ASL is particularly important in modulating the temperatures at Vernadsky. Figure 12c confirms the difference between the AP sub-regions in terms of the strength of the effect of the negative SLP anomaly. This is also a possible factor contributing to the NAP–SAP division by temperature trends.

As the tropical teleconnection in our results plays a much smaller role in the AP region in 2006–17 than SAM, it could be assumed that the negative SLP anomaly in the ASL region (Fig. 12c) presumably developed due to the positive SAM trend (Fig. S3a). Then, a deepening SLP anomaly and increasing SAM index are apparently responsible for the changing contribution from the zonal and meridional wind components to the surface temperature across the AP (Figs 9 & 10 & Table III).

In general, positive SAM polarity and negative SLP anomaly to the west of the AP region indicate regional cyclonic atmospheric circulation with warm northerly winds over the western AP (Kwok & Comiso 2002, Stammerjohn *et al.* 2008a, Yu *et al.* 2015, Clem *et al.* 2016, Turner *et al.* 2019). Negative regression between the northerly wind derived from the two reanalyses and observed temperature at FV is significant at the 95% confidence level (Fig. 10d). Along with the V-congruent component of the FV trend (although not significant statistically; Table III), this indicates that cooling in the SAP may be partly due to a decrease in the warm air transport from the north. Another part of the relative SAP cooling could be due to an insignificant contribution from the warm westerly wind (Fig. 10c) and more frequent contributions from the cold easterly wind observed in recent decades (Fig. 8b & c). In the NAP, the SAM effect is more persistent (Marshall 2007, Clem *et al.* 2016, Marshall & Thompson 2016) and is also seen from the SAM-congruent trend at ESP (Table III).

Distinct warming observed over the northern and southern parts of the AP was noted earlier and was related to changes in sea-ice cover (van Wessem *et al.* 2015) and at least partly to the temporally changing relationship between ENSO and SAM (Clem & Fogt

https://doi.org/10.1017/S0954102020000255 Published online by Cambridge University Press

2013, Clem *et al.* 2016, Marshall & Thompson 2016). Turner *et al.* (2019) note that some local wind systems can create regional sea-ice anomalies that have a large effect on temperatures over a small region, which can be independent of the large-scale variability. From our results, changes in the wind component combination in the NAP and SAP regions may also play a role. Changes in the zonal and meridional winds are associated with a development of the SLP anomaly to the west of the AP that, in turn, is dependent on the increasing positive SAM trend, as noted above. Obviously, the strength of the SLP anomaly and its shape directly along the AP (Fig. 12c) may influence the features of the atmospheric circulation here. As is known, the AP serves as an orographic barrier, modifying zonal and meridional winds (Marshall *et al.* 2006, Clem *et al.* 2016). The effect of this barrier gradually decreases towards the northern tip of the peninsula, and the zonal wind component prevails there. On the other hand, the recent deepening of the negative SLP anomaly closely adjacent to the SAP may contribute to a change in the local wind configuration, as seen in the increased frequency of the northerly wind at FV and ROT since the 2000s (Fig. 8b & c). Vernadsky is under the influence of the relatively warm climatological north-westerly flow (Turner *et al.* 2019), and a transition to the prevailing northerly winds that are becoming weaker may cause colder conditions. This assumption requires further study.

Conclusions

By analysing the decadal changes in the winter temperature on the AP, we found the existence of a difference between the NAP and SAP regions. The most noticeable difference is warming and cooling, respectively, in recent decades. Other recent analyses also show the different winter temperature trends on the NAP and SAP being closely tied to the changes in the ASL, which are associated with the ENSO–SAM relationship. Our results demonstrate the north–south asymmetry in the winter temperature trends in the 2000s–2010s from both the AP station records and the GISS Surface Temperature Analysis.

As established earlier, steady winter warming in the peninsula has occurred over the preceding five decades, from 1950 to 2000. From our results, the winter temperatures observed at the NAP and SAP stations (represented by ESP and FV, which were the longest-running data sets, having been collected since 1952 and 1951, respectively) are strongly correlated only during the 1980s and 1990s (Fig. 4). In this period, the temperature time series from both sets of stations are strongly correlated with the SST anomalies and zonal wind and geopotential height anomalies at 300 hPa in the central tropical Pacific around the N4 region, where Rossby wave trains propagate polewards from the tropics. The zonal wind anomalies along the wave train in the Pacific sector contain the zonally asymmetric component of the Annular Mode. Thus, remote (from the N4 region) and local (from the SAM) influences acted together in the 1980s and 1990s to favour the temperature co-variability over the entire AP region, with the most rapid warming occurring in both the NAP and SAP. Concurrent actions of the tropically forced and SAM-related impacts on AP warming are limited to these two decades, which is generally consistent with other studies. It should be emphasized that, in our analysis, the N4 and SAM indices in the winter are not correlated ($r \approx 0.1$); nevertheless, their independent but concurrent effects in the 1980s and 1990s led to rapid warming over the entire AP region.

The recent difference in the climate tendencies in the NAP and SAP is associated with a larger local contribution from the Annular Mode and a weakened effect of tropical anomalies, respectively. A similar spatial dependence in the ENSO and SAM influences on the decadal climate variability across the AP has been noted in other works. Mostly because of this dependence, a boundary arises that crosses the peninsula and divides it into sub-regions with warming and cooling.

Our results reveal that co-variability between the NAP and SAP station temperatures is greatly changing on the decadal timescale. It decreased to an insignificant level in the 1960s–1970s and has done again since the 2000s. In the last decade, the correlation temperature *vs* zonal wind field for ESP shows a prevailing SAM pattern with positive surface westerly anomalies at the NAP together with a wave 3 element. Both U-congruent and SAM-congruent components (with relatively low statistical significance) of the observed temperature trend at ESP suggest that the strengthening westerly wind associated with a positive shift in the SAM phase contributes to the recent NAP warming. The SAM impact is absent in the temperature change at FV, and the N4 region is partially coupled with the temperature variations and trend there in the last decade. Weakening warm northerly winds and the more frequent appearance of the cold easterly wind may also contribute to the recent SAP cooling.

It should be emphasized that positive temperature trends in the N4 and AP regions (Figs 3, 13 & S3b) are accompanied by negative temperature correlations (Fig. 5), and that warming or cooling in the AP sub-regions is mainly determined by trends in the local wind components (Figs 9 & 10).

Overall, the wind component relationship along the AP is influenced by the fixed AP orography and changing negative SLP anomaly in the ASL region, which is dependent on the zonal circulation strength. The rapid

https://doi.org/10.1017/S0954102020000255 Published online by Cambridge University Press

SAM shift to the positive phase in 2006–17 is a favourable factor for both the westerly wind strengthening and the negative SLP anomaly deepening. Westerly wind strengthening is unfavourable for tropical teleconnection, especially at the northern tip of the AP, where the winter wind speed is several times higher than in the SAP (as demonstrated by the observations and reanalysis data). These factors (the AP orography in combination with the SAM–negative SLP anomaly coupling) can configure the wind directions and influence their spatial variability in the AP region and thus introduce a difference between the SAP and NAP in terms of their wind component relationships; however, this assumption requires further study.

Acknowledgements

The authors thank the two anonymous referees for their valuable comments and helpful suggestions that improved our manuscript. We acknowledge the SCAR READER database for free access to the monthly data of the Antarctic station surface meteorology, available at www.antarctica.ac.uk/met/READER. The authors thank Jonathan Shanklin, Steve Colwell and Vladislav Tymofeyev for discussion on FV wind patterns. NCEP–NCAR reanalysis data and images are provided by the NOAA/OAR/ESRL PSD, Boulder, CO, USA, from their website at www.esrl.noaa.gov/psd. ERA-Interim reanalysis data were downloaded from the European Centre for Medium-Range Weather Forecasts (ECMWF) Public Datasets at https://apps.ecmwf.int/datasets. Marshall, G. & National Center for Atmospheric Research Staff (eds) provided SAM index (station-based) data, retrieved from https://climatedataguide.ucar.edu/climate-data/marshall-southern-annular-mode-sam-index-station-based. The temperature trend maps were used from the NASA GISS Surface Temperature Analysis at https://data.giss.nasa.gov/gistemp/maps.

Author contributions

OME conceived the work, participated in the data processing and wrote a part of the manuscript. VOK, AVG and GPM prepared statistical relationships and wrote parts of the manuscript. Each author contributed to the interpretation and discussion of the results and edited the manuscript.

Financial support

This work was supported by the project of Taras Shevchenko National University of Kyiv, No. 19BF051-08, and partly supported by the National Antarctic Scientific Center of Ukraine and by College of Physics, International Center of Future Science of Jilin University, China.

Supplemental material

Six supplemental figures and three supplemental tables will be found at https://doi.org/10.1017/S0954102020000255.

References

Carrasco, J.F. 2013. Decadal changes in the near-surface air temperature in the western side of the Antarctic Peninsula. *Atmospheric and Climate Sciences*, **3**, 10.4236/acs.2013.33029.

Clem, K.R. & Fogt, R.L. 2013. Varying roles of ENSO and SAM on the Antarctic Peninsula climate in austral spring. *Journal of Geophysical Research – Atmospheres*, **118**, 10.1002/jgrd.50860.

Clem, K.R., Renwick, J.A. & McGregor, J. 2017. Large-scale forcing of the Amundsen Sea Low and its influence on sea ice and West Antarctic temperature. *Journal of Climate*, **30**, 10.1175/JCLI-D-16-0891.1.

Clem, K.R., Renwick, J.A., McGregor, J. & Fogt, R.L. 2016. The relative influence of ENSO and SAM on Antarctic Peninsula climate. *Journal of Geophysical Research – Atmospheres*, **121**, 10.1002/2016JD025305.

Dee, D.P., Uppala, S.M., Simmons, A.J., Berrisford, P., Poli, P., Kobayashi, S., *et al.* 2011. The ERA-Interim reanalysis: configuration and performance of the data assimilation system. *Quarterly Journal of the Royal Meteorological Society*, **137**, 10.1002/qj.828.

Ding, Q. & Steig, E.J. 2013. Temperature change on the Antarctic Peninsula linked to the tropical Pacific. *Journal of Climate*, **26**, 7570–7585.

Ding, Q., Steig, E.J., Battisti, D.S. & Küttel, M. 2011. Winter warming in West Antarctica caused by central tropical Pacific warming. *Nature Geoscience*, **4**, 10.1038/ngeo1129.

Ding, Q., Steig, E.J., Battisti, D.S. & Wallace, J.M. 2012. Influence of the tropics on the Southern Annular Mode. *Journal of Climate*, **25**, 6330–6348.

Fogt, R.L. & Bromwich, D.H. 2006. Decadal variability of the ENSO teleconnection to the high-latitude South Pacific governed by coupling with the Southern Annular Mode. *Journal of Climate*, **19**, 979–997.

Fogt, R.L., Wovrosh, A.J., Langen, R.A. & Simmonds, I. 2012. The characteristic variability and connection to the underlying synoptic activity of the Amundsen–Bellingshausen Seas Low. *Journal of Geophysical Research – Atmospheres*, **117**, 10.1029/2011JD017337.

Hansen, J., Ruedy, R., Sato, M. & Lo, K. 2010. Global surface temperature change. *Reviews of Geophysics*, **48**, 10.1029/2010RG000345.

Kalnay, E., Kanamitsu, M., Kistler, R., Collins, W., Deaven, D., Gandin, L., *et al.* 1996. The NCEP–NCAR 40-year reanalysis project. *Bulletin of the American Meteorological Society*, **77**, 1057–1072.

King, J.C. 1994. Recent climate variability in the vicinity of the Antarctic Peninsula. *International Journal of Climatology*, **14**, 357–369.

King, J.C. & Comiso, J.C. 2003. The spatial coherence of interannual temperature variations in the Antarctic Peninsula. *Geophysical Research Letters*, **30**, 10.1029/2002GL015580.

Kravchenko, V.O., Evtushevsky, O.M., Grytsai, A.V. & Milinevsky, G.P. 2011. Decadal variability of winter temperatures in the Antarctic Peninsula region. *Antarctic Science*, **23**, 614–622.

Kushner, P.J., Held, I.M. & Delworth, T.L. 2001. Southern Hemisphere atmospheric circulation response to global warming. *Journal of Climate*, **14**, 2238–2249.

Kwok, R. & Comiso, J.C. 2002. Spatial patterns of variability in Antarctic surface temperature: connections to the Southern Hemisphere Annular Mode and the Southern Oscillation. *Geophysical Research Letters*, **29**, 10.1029/2002GL015415.

Marshall, G.J. 2003. Trends in the Southern Annular Mode from observations and reanalyses. *Journal of Climate*, **16**, 4134–4143.

Marshall, G.J. 2007. Half-century seasonal relationships between the Southern Annular Mode and Antarctic temperatures. *International Journal of Climatology*, **27**, 373–383.

Marshall, G.J. & Thompson, D.W.J. 2016. The signatures of large-scale patterns of atmospheric variability in Antarctic surface temperatures. *Journal of Geophysical Research – Atmospheres*, **121**, 10.1002/2015JD024665.

Marshall, G.J., Orr, A., van Lipzig, N.P.M. & King, J.C. 2006. The impact of a changing Southern Hemisphere Annular Mode on Antarctic Peninsula summer temperatures. *Journal of Climate*, **19**, 5388–5404.

Mo, K.C. 2000. Relationships between low-frequency variability in the Southern Hemisphere and sea surface temperature anomalies. *Journal of Climate*, **13**, 3599–3610.

Oliva, M., Navarro, F., Hrbáček, F., Hernández, A., Nývlt, D., Pereira, P., *et al*. 2017. Recent regional climate cooling on the Antarctic Peninsula and associated impacts on the cryosphere. *Science of the Total Environment*, **580**, 210–223.

Raphael, M.N. 2004. A zonal wave 3 index for the Southern Hemisphere. *Geophysical Research Letters*, **31**, 10.1029/2004GL020365.

Raphael, M.N., Marshall, G.J., Turner, J., Fogt, R.L., Schneider, D., Dixon, D.A., *et al*. 2016. The Amundsen Sea Low: variability, change, and impact on Antarctic climate. *Bulletin of the American Meteorological Society*, **97**, 10.1175/BAMS-D-14-00018.1.

Schneider, D.P., Deser, C. & Okumura, Y. 2012. An assessment and interpretation of the observed warming of West Antarctica in the austral spring. *Climate Dynamics*, **38**, 323–347.

Seidel, D.J. & Lanzante, J.R. 2004. An assessment of three alternatives to linear trends for characterizing global atmospheric temperature changes. *Journal of Geophysical Research – Atmospheres*, **109**, 10.1029/2003JD004414.

Stammerjohn, S.E., Martinson, D.G., Smith, R.C. & Iannuzzi, R.A. 2008a. Sea ice in the western Antarctic Peninsula region: spatio-temporal variability from ecological and climate change perspectives. *Deep-Sea Research II*, **55**, 10.1016/j.dsr2.2008.04.026.

Stammerjohn, S.E., Martinson, D.G., Smith, R.C., Yuan, X. & Rind, D. 2008b. Trends in Antarctic annual sea ice retreat and advance and their relation to El Niño–Southern Oscillation and Southern Annular Mode variability. *Journal of Geophysical Research*, **113**, 10.1029/2007JC004269.

Stastna, V. 2010. Spatio-temporal changes in surface air temperature in the region of the northern Antarctic Peninsula and South Shetland Islands during 1950–2003. *Polar Science*, **4**, 18–33.

Thompson, D.W.J. & Solomon, S. 2002. Interpretation of recent Southern Hemisphere climate change. *Science*, **296**, 895–899.

Thompson, D.W.J., Wallace, J.M. & Hegerl, G.C. 2000. Annular modes in the extratropical circulation. Part II: trends. *Journal of Climate*, **13**, 1018–1036.

Thompson, D.W.J., Solomon, S., Kushner, P.J., England, M.H., Grise, K.M. & Karoly, D.J. 2011. Signatures of the Antarctic ozone hole in Southern Hemisphere surface climate change. *Nature Geoscience*, **4**, 741–749.

Turner, J., Phillips, T., Hosking, J.S., Marshall, G.J. & Orr, A. 2013. The Amundsen Sea Low. *International Journal of Climatology*, **33**, 10.1002/joc.3558.

Turner, J., Marshall, G.J., Clem, K., Colwell, S., Phillips, T. & Lu, H. 2019. Antarctic temperature variability and change from station data. *International Journal of Climatology*, 10.1002/joc.6378.

Turner, J., Colwell, S.R., Marshall, G.J., Lachlan-Cope, T.A., Carleton, A.M., Jones, P.D., *et al*. 2004. The SCAR READER project: toward a high-quality database of mean Antarctic meteorological observations. *Journal of Climate*, **17**, 2890–2898.

Turner, J., Colwell, S.R., Marshall, G.J., Lachlan-Cope, T.A., Carleton, A.M., Jones, P.D., *et al*. 2005. Antarctic climate change during the last 50 years. *International Journal of Climatology*, **25**, 279–294.

Turner, J., Lu, H., White, I., King, J.C., Phillips, T., Hosking, J.S., *et al*. 2016. Absence of 21st century warming on Antarctic Peninsula consistent with natural variability. *Nature*, **535**, 411–415.

Tymofeyev, V.E. 2014. Some peculiarities of the near-surface air temperature change in the Antarctic Peninsula region. *Ukrainian Antarctic Journal*, **13**, 110–123.

van Wessem, J., Reijmer, C.H., van de Berg, W.J., van den Broeke, M.R., Cook, A.J., van Ulft, L.H., *et al*. 2015. Temperature and wind climate of the Antarctic Peninsula as simulated by a high-resolution regional atmospheric climate model. *Journal of Climate*, **28**, 7306–7326.

Vaughan, D.G., Marshall, G.J., Connolley, W.M., Parkinson, C., Mulvaney, R., Hodgson, D.A., *et al*. 2003. Recent rapid regional climate warming on the Antarctic Peninsula. *Climatic Change*, **60**, 243–274.

Wang, Y., Zhou, D., Bunde, A. & Havlin, S. 2016. Testing reanalysis data sets in Antarctica: trends, persistence properties, and trend significance. *Journal of Geophysical Research – Atmospheres*, **121**, 10.1002/2016JD024864.

Yang, X.-Y., Yuan, X. & Ting, M. 2016. Dynamical link between the Barents–Kara Sea ice and the Arctic Oscillation. *Journal of Climate*, **29**, 5103–5122.

Yu, J.Y., Paek, H., Saltzman, E.S. & Lee, T. 2015. The early 1990s change in ENSO–PSA–SAM relationships and its impact on Southern Hemisphere climate. *Journal of Climate*, **28**, 10.1175/JCLI-D-15-0335.1.

Yu, L., Zhong, S. & Sun, B. 2020. The climatology and trend of surface wind speed over Antarctica and the Southern Ocean and the implication to wind energy application. *Atmosphere*, **11**, 10.3390/atmos11010108.

Yu, L., Zhang, Z., Zhou, M., Zhong, S., Lenschow, D., Hsu, H., *et al*. 2012. Influence of the Antarctic Oscillation, the Pacific–South American modes and the El Niño–Southern Oscillation on the Antarctic surface temperature and pressure variations. *Antarctic Science*, **24**, 10.1017/S095410201100054X.

Yuan, X. & Li, C. 2008. Climate modes in southern high latitudes and their impacts on Antarctic sea ice. *Journal of Geophysical Research – Oceans*, **113**, 10.1029/2006JC004067.

Yuan, X. & Martinson, D.G. 2001. The Antarctic Dipole and its predictability. *Geophysical Research Letters*, **28**, 3609–3612.

Yuan, X., Kaplan, M. & Cane, M. 2018. The interconnected global climate system – a review of tropical–polar teleconnections. *Journal of Climate*, **31**, 10.1175/JCLID-16-0637.1.